Efficient Azimuthal Mode Analysis using Compressed Sensing

Maximilian Behn *, Roman Kisler † and Ulf Tapken ‡

German Aerospace Center (DLR), Institute of Propulsion Technology, Berlin, Germany

A new approach for the Azimuthal Mode Analysis (AMA) of over- and subsampled sound fields in flow ducts of turbomachines using circumferential sensor arrays is presented which is based on Compressed Sensing. Compressed Sensing is a framework to solve underdetermined systems of linear equations under the assumption that the solution vector is sparse. In the context of AMA, such sparse mode spectra often occur in the analysis of tonal sound field components generated by rotor-stator interaction. Important features such as stability and accuracy are investigated by analysis of a wide range of simulated and measured pressure data and comparison with commonly applied methods. Also two different optimisation approaches for the design of circumferential sensor arrays are introduced which allows a reduction of the number of sensors for large modal ranges if only a limited number of modes are dominant. Furthermore, the remaining mode amplitudes are estimated exploiting the deconvolution property of the applied Compressed Sensing algorithm.

I. Introduction

THE experimental investigation of in-duct sound fields in turbomachinery test rigs presents manifold challenges towards the design of the experiment. The decomposition of the azimuthal pressure distribution into azimuthal mode constituents requires measurements at several locations around the circumference[1]. For a subsequent breakdown into radial modes the measurements have to be extended to several radial resp. axial positions[2]. The choice of the number and positioning of the sensors in an array plays a critical role. The usual task is to ensure a sufficient spatial resolution and a low side lobe level (SLL) for a given number of sensors. Therefore, it is of interest to investigate methods that allow the reduction of the required number of sensors for a given modal range. There are several approaches to find the best compromise between the spatial resolution, the analysis accuracy and the number of sensors resulting in different guidelines for the design of optimal sensor arrays.

In this paper a new approach to Azimuthal Mode Analysis (AMA) based on Compressed Sensing (CS) is presented and the improvements compared to the conventional methods[3,4] are discussed. Compressed Sensing is predestined for solving underdetermined systems of linear equations in the case of a sparse mode spectrum and offers a large potential to detect the dominant mode amplitudes with a limited number of sensors. The approach is similar to the one described by Huang[5] who performed a numerical study using randomised array designs, except for the choice of the CS algorithm. Additionally, a deconvolution step is introduced to enable the determination of the amplitudes of the entire mode spectrum under consideration. In order to exploit the full potential of the proposed method an optimisation criterion for the design of the sensor array is described Two different approaches to find the optimal array design are introduced. Results are shown for simulated test cases as well as measured data sensed by an optimised array. To the authors' knowledge, there are very few cases in literature that describe the use of Compressed Sensing in in-duct sound measurements to date. For instance, Lengani et al.[6] used a Compressed-Sensing based approach

*Research Engineer, Engine Acoustics Department, Müller-Breslau-Straße 8, 10623 Berlin, Germany, maximilian.behn@dlr.de
†Master Student, Engine Acoustics Department, Müller-Breslau-Straße 8, 10623 Berlin, Germany
‡Research Scientist, Engine Acoustics Department, Müller-Breslau-Straße 8, 10623 Berlin, Germany, ulf.tapken@dlr.de

to determine a sparse approximation of the azimuthal mode spectrum from measurements with wall flush-mounted microphones on a 24° circumference and gave an empirical error estimation.

The paper is divided into four sections. Beginning with the introduction of the related equations for AMA, the conventional methods are described and the new approach for Compressed Sensing based AMA is presented along with the introduction of the deconvolution step. Following, the optimisation of array designs for the application in the context of CS is discussed. The methods are applied to simulated and measured data and the features of the new approach are investigated.

II. Methods for the Azimuthal Mode Analysis

The Azimuthal Mode Analysis can be derived from the general solution in modal terms of the convective Helmholtz equation in cylindrical coordinates[4]:

$$p(x,r,\varphi) = \sum_{m=-\infty}^{+\infty} \sum_{n=0}^{+\infty} \left(A_{mn}^{+} \cdot e^{ik_{mn}^{+}x} + A_{mn}^{-} \cdot e^{ik_{mn}^{-}x} \right) \cdot f_{mn}(r) \cdot e^{im\varphi} \tag{1}$$

for time-harmonic waves. In Eq. (1), k_{mn}^{+} and k_{mn}^{-} are the axial wave numbers, A_{mn}^{+} and A_{mn}^{-} the complex amplitudes of the radial modes with azimuthal mode order m and radial mode order n propagating downstream and upstream, respectively. The term $f_{mn}(r)$ denotes the radial mode shape factor which is determined by the flow parameters and the duct geometry.

Denoting the value of the sum over all radial mode orders n for fixed azimuthal mode order m as the complex azimuthal mode amplitude A_m, the decomposition of the sound field in azimuthal modes yields:

$$p(x,\varphi) = \sum_{m=-\infty}^{+\infty} A_m(x) \cdot e^{im\varphi}. \tag{2}$$

The radial dependency is neglected under the assumption that the decomposition is based on measurements with wall flush-mounted sensors. At a fixed axial position $\hat{x}$ the azimuthal mode spectrum is determined by the Fourier transform of the sound pressure with respect to the azimuthal coordinate:

$$A_m = \frac{1}{2\pi} \int_0^{2\pi} p(\hat{x},\varphi) \cdot e^{-im\varphi} \, \mathrm{d}\varphi. \tag{3}$$

In an experimental context sparse arrays are applied, so that the integral in Eq. (3) is replaced by a sum over the sensor positions φ_k yielding the expression for the Discrete Fourier Transform (DFT):

$$A_m = \frac{1}{K} \sum_{k=1}^{K} p(\hat{x},\varphi_k) \cdot e^{-im\varphi_k}. \tag{4}$$

The relation between the complex sound pressure values $\boldsymbol{p}$ measured at K sensor positions and the underlying azimuthal mode spectrum $\boldsymbol{a}$, where M propagating modes are considered, can be formulated as a system of linear equations:

$$\boldsymbol{p} = \boldsymbol{W}\boldsymbol{a} \tag{5}$$

where $\boldsymbol{W}$ is a matrix of size KxM with the mode functions evaluated for the mth mode order at the kth sensor position as entries (see Eq. (4)). In this study the modal range is always symmetrical w.r.t. $m = 0$, i.e. $m \in \{-m_{max}, \cdots, 0, \cdots, m_{max}\}$ with a total number of modes $M = 2 \cdot m_{max} + 1$. The Azimuthal Mode Analysis is performed by solving the system of linear equations in Eq. (5).

II.A. Conventional Methods

There exist a number of methods to determine the azimuthal mode spectrum, i.e. to solve Eq. (5)[1,8,3,9,10], but the most commonly applied methods are a least-squares fit (LSF) and the Discrete Fourier Transform

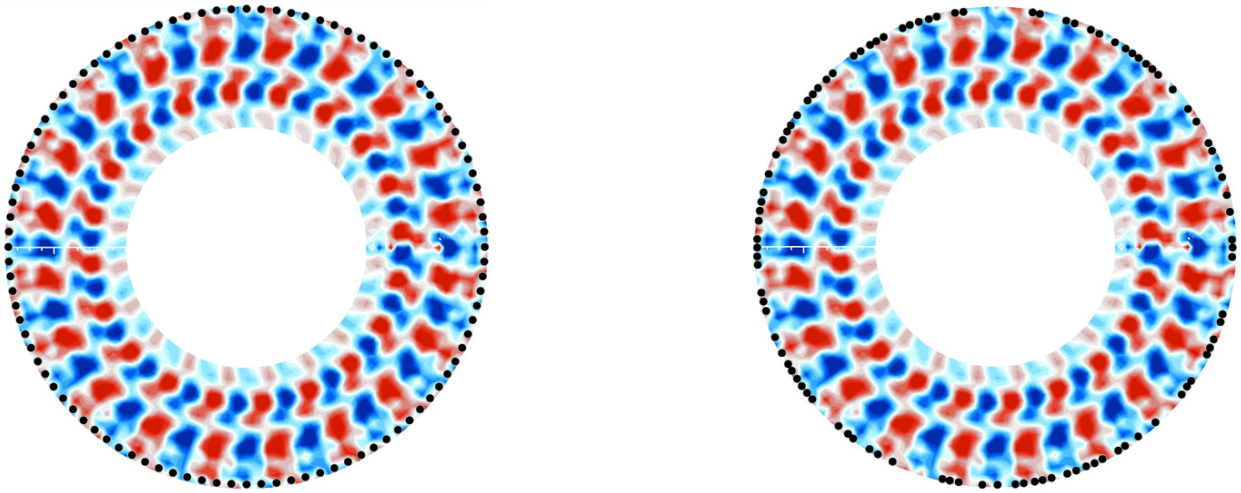

(a) Uniform array (b) Non-uniform array

Figure 1. Illustration of the Azimuthal Mode Analysis using a uniform resp. a non-uniform array consisting of 100 sensors at the wall of a flow duct with a simulated sound field. Black dots indicate sensor positions. The non-uniform array design is implemented in the CMD arrays[7] of the UFFA test rig of AneCom Aerotest, Germany.

(DFT). Applying LSF to Eq. (5) yields in matrix-vector notation:

$$\boldsymbol{a} = \left[\boldsymbol{W}^H \boldsymbol{W}\right]^{-1} \boldsymbol{W}^H \boldsymbol{p}, \tag{6}$$

where the superscript H denotes the adjoint matrix. The term $\left[\boldsymbol{W}^H \boldsymbol{W}\right]^{-1} \boldsymbol{W}^H$ is called the pseudo-inverse of matrix $\boldsymbol{W}$. Applying the pseudo-inverse to the sound pressure vector $\boldsymbol{p}$ results in a mode amplitude vector which minimises the l2-norm of the residuum according to the cost function $J = \|\boldsymbol{e}\|_2 = \|\boldsymbol{W}\boldsymbol{a} - \boldsymbol{p}\|_2$.
In matrix-vector notation the DFT takes the form:

$$\boldsymbol{a} = \frac{1}{K} \boldsymbol{W}^H \boldsymbol{p}. \tag{7}$$

Both methods, LSF and DFT, perform well in cases where the number of sensors K is larger than the number of propagating modes M and the sensors are equally spaced along the circumference. In the described case of oversampling, the system of linear equations in Eq. (5) is overdetermined and the approaches in Eq. (6) and (7) yield the exact solution vector of the mode spectrum.

However, if the sound field is undersampled, then typically aliasing effects occur, which can hamper the interpretation of the mode spectrum. The aliasing effects can be avoided by arranging the sensors with non-uniform spacing, but with drawback of the occurrence of side lobes even for oversampled sound fields. Rademaker et al.[3] proposed a cost function which can be used in an optimisation of non-uniform arrays, which minimises the mean square of the side lobe amplitudes for the analysis of a number of modes M larger than the number of sensors K. Illustrations of a uniform resp. a non-uniform array applied in the context of AMA are shown in figure 1.

II.B. Compressed Sensing based Azimuthal Mode Analysis

Compressed Sensing is an approach for solving underdetermined systems of linear equations under the assumption that the solution vector is sparse, i.e. the azimuthal mode spectrum consists only of a few dominant modes. The analysis of the interaction tones of a rotor-stator stage in a turbomachine is an example, where sparse azimuthal mode spectra with dominant modes, also called Tyler-Sofrin modes[11], occur. In practice, the microphone signals are influenced by superposed noise components due to e.g. turbulent flow noise and thus, the mode spectra show additional modes aside from the Tyler-Sofrin modes. Typically, the Tyler-Sofrin modes have significantly higher levels than the noise related components of the mode spectrum. In

such cases, it is assumed that the mode spectrum is compressible, i.e. the sound pressure pattern at the microphones is well-approximated by the contribution of the dominant modes[12].

Given the sparsity of the mode amplitude vector the correct solution can be found by minimising the l1-norm of the solution vector[13,14]. In terms of AMA with an assumed noise energy ϵ this can be formulated mathematically as follows:

$$\boldsymbol{a} = \underset{\boldsymbol{a}\in\mathbb{C}^M}{\operatorname{argmin}} \|\boldsymbol{a}\|_1 \quad \text{subject to } \|\boldsymbol{p} - \boldsymbol{W}\boldsymbol{a}\|_2 < \epsilon. \tag{8}$$

The minimisation problem can be solved in various ways. In the present study a so-called Greedy Algorithm[12] is applied. This class of algorithms contains iterative algorithms which update the mode amplitude vector regarding the best sparse approximation of the solution vector of Eq. (5) at each iteration. Particularly, the utilised Orthogonal Matching Pursuit algorithm (OMP), which was first proposed to be applied in the context of Compressed Sensing by Tropp and Gilbert[15], searches for the modes with th highest amplitudes until a convergence or stop criterion is met. Thus, after s iterations the strongest s modes are determined in the mode amplitude vector $\boldsymbol{a}^{(s)}$. The superscript s stands for the iteration count and also indicates the number of determined modes. An interesting aspect of the iterative procedure of OMP is, that the contribution of each newly determined mode is deconvolved from the sound pressure vector at each iteration. This feature of the OMP-algorithm is exploited in the next section in order to estimate the remaining mode spectrum.

Eldar and Kutyniok[12] mention that sparse recovery by minimisation of the l1-norm is successful, if the column vectors of the system matrix $\boldsymbol{W}$ are incoherent. The mutual coherence μ of the matrix W is defined as:

$$\mu(\boldsymbol{W}) = \max_{1\leq i<j\leq M} \frac{|\langle \boldsymbol{w}_i, \boldsymbol{w}_j\rangle|}{\|\boldsymbol{w}_i\|_2\|\boldsymbol{w}_j\|_2} \tag{9}$$

where $\boldsymbol{w}_i$ denotes the ith column vector of $\boldsymbol{W}$. Since the system matrix $\boldsymbol{W}$ only depends on the modal range and the positions of the sensors in the microphone array, the mutual coherence can be regarded as a property of the sensor array. For a configuration with K microphones and M modes, the mutual coherence lies within the range $\mu(\boldsymbol{W}) \in \left[\sqrt{\frac{M-K}{K(M-1)}}, 1\right]$. The lower bound is called Welch bound and depends only on the size of matrix $\boldsymbol{W}$. A small value of the mutual coherence indicates that any pair of column vectors has a small value of the normalised inner product and therefore, the respective column vectors are close to orthogonal. The error between the exact solution and the calculated mode spectrum is smaller the lower the mutual coherence of an array. This is true, if the number of determined mode amplitudes s fulfills the inequality $s < \frac{1}{\mu(\boldsymbol{W})}$. Furthermore, the mutual coherence is directly linked to the side lobe level (SLL)[16], which is a common parameter in the theory of sensor arrays, according to following equation:

$$\mathrm{SLL} = 20\log_{10}\left(\frac{1}{\mu(\boldsymbol{W})}\right). \tag{10}$$

The ability of Compressed Sensing to solve underdetermined systems of linear equations provides potential to reduce the number of sensors in a circumferential sensor array. Figure 2 shows the number of dominant modes which are detectable depending on the modal range and the number of sensors. The results are given for optimal arrays which achieve the Welch bound. In the coloured region the sound field is subsampled and it holds that $K < M$. The white region indicates the configurations for which the sound field is oversampled and all mode amplitudes within the modal range can be determined accurately as shown in section IV. As an example the required numbers of sensors for the detection of 5 resp. 20 dominant modes are indicated by black lines. It can be observed, that if few dominant modes are of interest the potential to reduce the number of sensors becomes large. For instance, if $s = 5$ the required number of sensors increases very slowly with larger modal ranges and asymptotically approaches the value of 24 sensors for modal ranges up to $M = 400$, i.e. the ratio of modes per sensor yields $\gamma = M/K \approx 16.7$.

II.C. Estimation of the remaining mode spectrum by deconvolution with the sparse mode spectrum

As described above, the Azimuthal Mode Analysis based on Compressed Sensing allows the determination of a number of dominant modes depending on the mutual coherence of the applied sensor array. During the iterative procedure of the OMP-algorithm the sound pressure vector is successively deconvolved with the

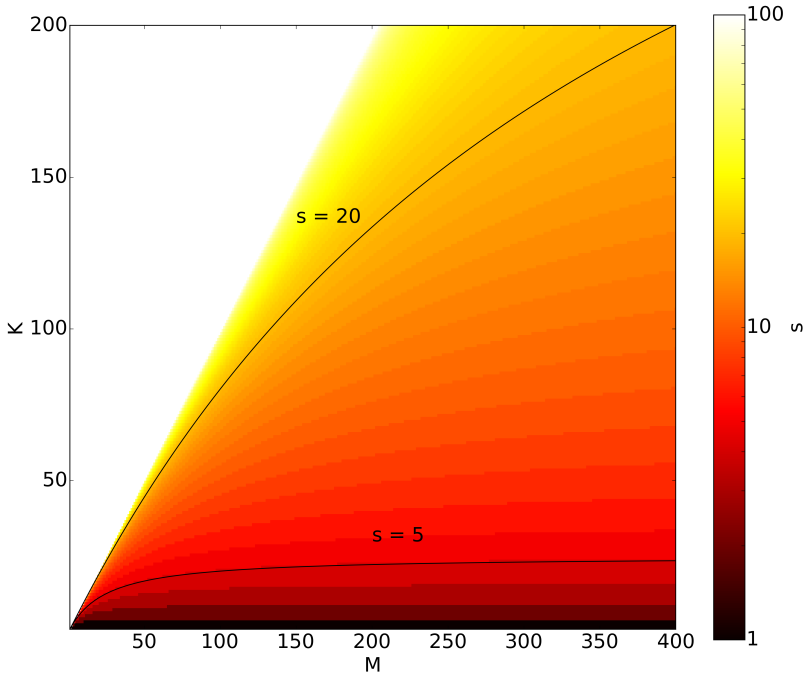

Figure 2. Number of detectable, dominant modes s by use of Compressed Sensing depending on the number of modes M and number of sensors K.

determined mode amplitudes. After the termination of the OMP-algorithm an additional calculation step using the deconvolved sound pressure vector $\boldsymbol{p}^s$ leads to a good estimation of the remaining mode spectrum. This method is called Enhanced OMP (EOMP) within the scope of this study. The additional calculation step consists of solving the following equation:

$$\boldsymbol{p}^{(s)} = \boldsymbol{W}\boldsymbol{a}^{(M-s)} \tag{11}$$

by use of the LSF- or DFT-method. Hereby, the choice between LSF and DFT depends on the ratio of the number of modes and the number of microphones γ. If $\gamma < 1$ the system of linear equations in Eq. (5) is overdetermined and LSF can be applied provided that the condition number of W is small. If the condition number of the system matrix reaches high values, small errors in the measurement vector, i.e. the vector $\boldsymbol{p}$ on the left-hand side in Eq. (5), are amplified and corrupt the resulting mode amplitude vector $\boldsymbol{a}$. Thus, in order to ensure a stable behaviour of the EOMP-method the DFT-method is applied for the deconvolution step. For $\gamma > 1$ the problem is underdetermined and DFT is the appropriate choice. Results using the described deconvolution procedure are shown and discussed in section IV. Finally, the two determined mode amplitude vectors are summed to form the total mode amplitude vector:

$$\boldsymbol{a}_{total} = \boldsymbol{a}^{(s)} + \boldsymbol{a}^{(M-s)}. \tag{12}$$

III. Design of optimal arrays for application of the Compressed Sensing algorithm

The application of CS in an experimental setup raises the need for guidelines for the design of optimal arrays. Often randomised arrays are used in the context of Compressed Sensing. In this study two approaches for the design of optimal arrays are introduced. The first approach is deterministic and is based on the definition of the mutual coherence of matrix $\boldsymbol{W}$. Inserting the entries of the column vectors $\boldsymbol{w}_{i,j}$ and evaluating the inner products in Eq. (9) yields following equation:

$$F := \min \mu(\boldsymbol{W}) \tag{13}$$

$$= \min \max_{\Delta m \in \{1,\dots,M-1\}} \frac{\left|\sum_{k=1}^{K} \exp(i\Delta m \varphi_k)\right|}{K}. \tag{14}$$

By minimisation of Eq. (14) with respect to the sensor positions φ_k of all K sensors an optimal array can be determined. It turns out, that the optimisation procedure of Rademaker et al[3] results in array geometries that yield similar values of the mutual coherence for large arrays. Furthermore, the functional in Eq. (14) becomes equal to the Rademaker functional, if the maximum operator is replaced by the mean square. Due to the connection of the mutual coherence and the side lobe level (see Eq. (10)) the proposed functional minimises the maximum side lobe amplitude. An array which was designed following the method of Rademaker et al. is installed in the UFFA rig of AneCom AeroTest, Germany[7].

The second approach follows the postulation of Xia et al.[17], who proposed that so-called Welch bound arrays with K sensors are subsets of a uniform array with $K_{eq} = M$. The optimisation approach comprises the random selection of subsets from a large uniform array. This approach is efficient for small K and M, but becomes tedious for large array sizes and mode ranges commonly considered in practical applications. It should be noted at this point, that due to the choice of subsets from a uniform array, a strict limit regarding the applicable modal range exists. If the applied modal range exceeds the modal range for which the array is optimised, the mutual coherence achieves values of 1 due to aliasing and the reconstruction of the azimuthal mode spectrum is impaired.

The resulting mutual coherence of a particular array can be visualised by plotting the normalised inner products according to Eq. (9). Due to the structure of the column vectors of matrix $\boldsymbol{W}$ the mutual coherence needs only to be plotted over the first M inner products. In figure 3 the coherences of each pair of modes of an optimised array according to Eq. (14) and a randomised array are shown. The optimised array yields approximately equal values for the normalised inner products from Eq. (9), which also implies that the measurement error is similar for each analysed mode. On the contrary, the normalised inner products for the random array show a relatively large deviation and peaks for certain pairs of analysed modes. Thus, a reconstructed mode spectrum would have a varying analysis error depending on the coherence between each possible pair of modes and the input mode spectrum.

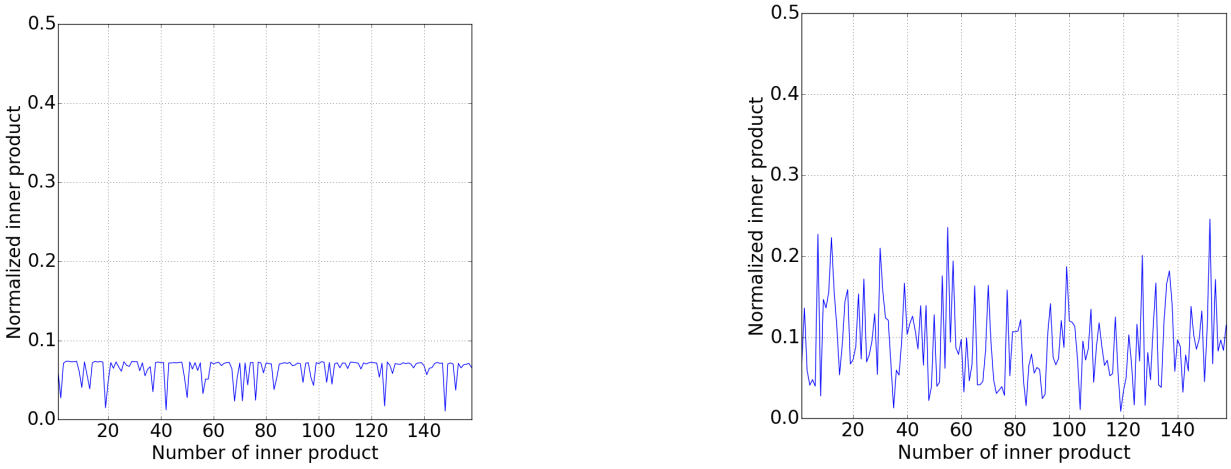

(a) Optimal

(b) Random

Figure 3. Comparison of the normalised inner products of the column vectors of the system matrix $\boldsymbol{W}$ of the optimised CMD array at the UFFA test rig (see figure 1b) and a random array ($K = 100$, $M = 159$).

In addition to the described optimisation approaches, a Monte Carlo study was conducted to investigate the properties of arbitrary arrays (Type I) and arrays, which are subsets of a large uniform array with $K = M$ sensors (Type II). The study was performed for arrays with $K = 100$ sensors, a modal range with $M = 159$ and 10,000 trials. The histogram in figure 4 shows the distributions of the relative frequency of the mutual coherence for both types of arrays. It can be seen, that with high probability arrays of Type II have a lower mutual coherence and thus, choosing arrays of Type II as a starting point for the optimisation procedure according to Eq. (14) yields better results. The Welch bound is indicated by the blue vertical line. None of the considered arrays achieves the Welch bound, but more than 90% of the Type II arrays

perform better than the arbitrary arrays and achieve a mutual coherence close to the Welch bound. Furthermore, this empirical study supports the general idea of the stochastic optimisation approach described above.

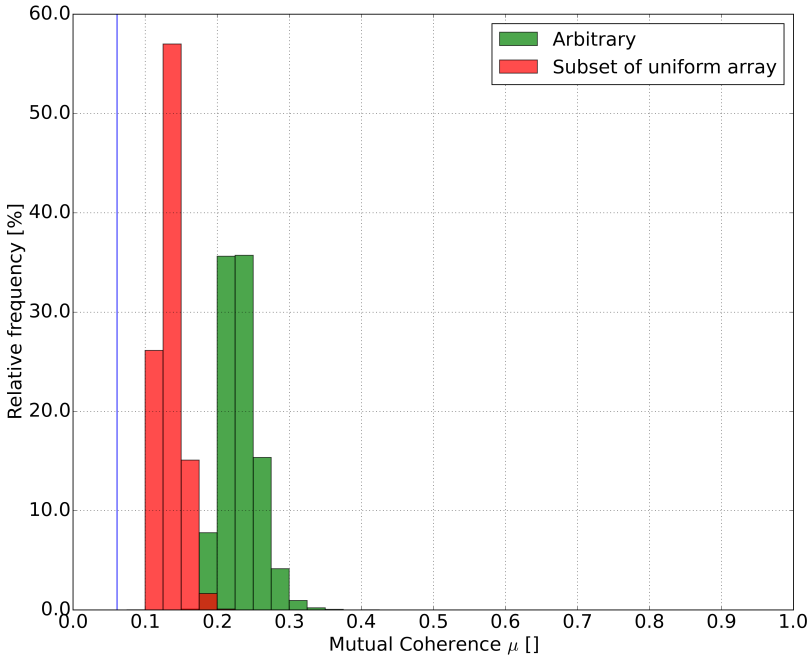

Figure 4. Relative frequency of the mutual coherence of arbitrary arrays and subset arrays of a large uniform array ($K = 100$, $M = 159$).

IV. Comparison of analysis methods

In the following section, the properties of the presented method are studied by application to simulated and measurement data. Two cases, oversampled ($K > M$) and subsampled ($K < M$) test setups, are investigated. The focus of the present study is put on the differences between Compressed Sensing based AMA and the conventional methods, LSF and DFT. At first, important characteristics of the presented method are determined by analysis of mode spectra with arbitrary resp. specific phase relations. Subsequently, this information is applied to evaluate the quality of the analysis of experimental data.

IV.A. Application to simulated data

The procedure for the following analyses of simulated data has been developed with the aim to simulate data from practical measurements appropriately. A number of dominant modes is given and the orders of the respective modes are assigned randomly. Subsequently, modes with random phase and signal-to-noise ratio (SNR) of about 30 dB are added to the input mode spectrum. The study presents results for two configurations, where the first configuration is overdetermined with $K = 100$ and $M = 99$ and the second configuration is underdetermined with $K = 100$ and $M = 159$. For each setup the design of the CMD array is used, which is illustrated in figure 1b and implemented in the UFFA test rig of AneCom AeroTest, Germany. The UFFA test rig is depicted in figure 5.

IV.A.1. Reconstruction of mode spectra with arbitrary phase relations

In figures 6 and 7 results of LSF, DFT and Compressed Sensing based AMA with and without the additional deconvolution step are shown for a simulated measurement with a non-uniform array of 100 sensors. In the original spectrum 11 dominant modes of random mode orders are present. The average sound pressure level

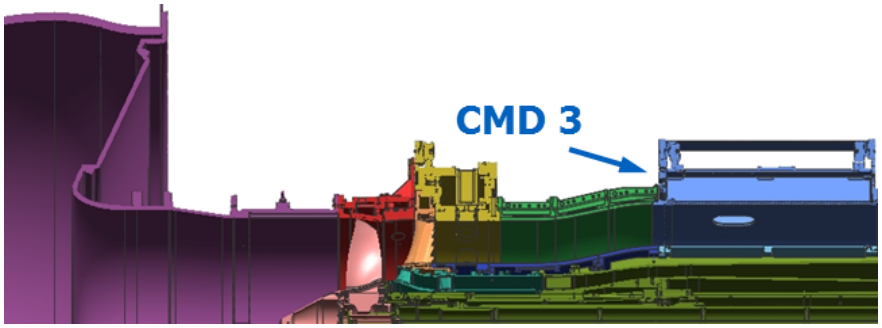

Figure 5. Test setup for the measurements of azimuthal mode spectra using a non-uniform array (CMD 3) in the downstream by-pass duct of the UFFA test rig of AneCom AeroTest, Germany.

SPL_{avg} is calculated based on the sound pressure level of the azimuthal modes SPL_m using

$$\mathrm{SPL}_{avg} = 10 \cdot \log_{10}\left(\frac{1}{M}\sum_{m=-m_{max}}^{m_{max}} 10^{\mathrm{SPL}_m/10}\right) \tag{15}$$

and indicated by the red horizontal lines. For both cases the average sound pressure level is about 17 dB below the amplitude of the most dominant mode.

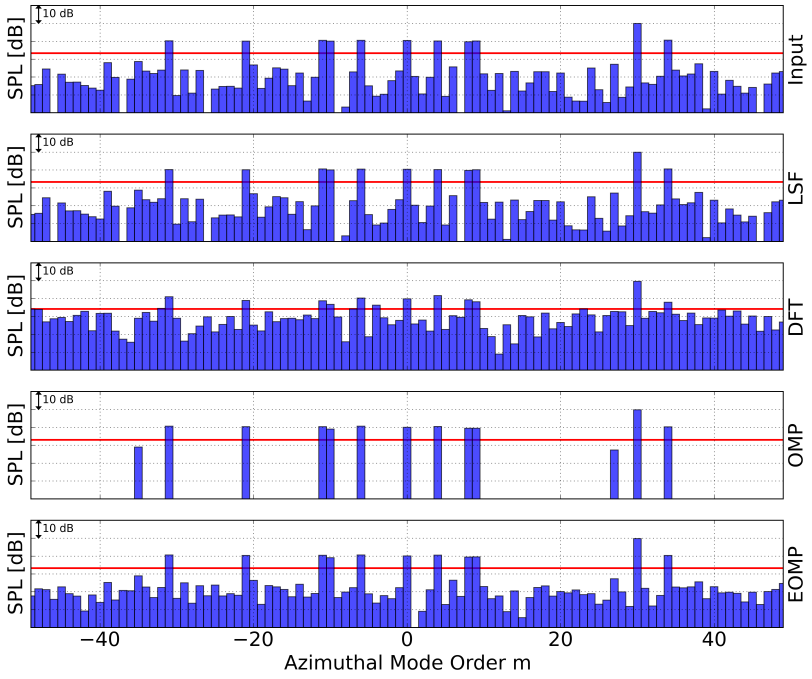

Figure 6. Results of different azimuthal mode analysis methods applied to a simulated pressure data set. The underlying mode spectrum has arbitrary phase relations. For each analysis of the sound field consisting of $M = 99$ azimuthal modes the same sensor array consisting of $K = 100$ unequally spaced sensors was used.

In the case of oversampling the sound field, all methods give approximately the correct average sound pressure level. However, only the LSF algorithm reconstructs the mode spectrum perfectly. The Compressed Sensing based methods, OMP and EOMP, determine all dominant modes correctly. Also EOMP is able to estimate the mode amplitudes below the average sound pressure level with great precision. The amplitudes of the dominant modes are determined well by the DFT-method, but it fails to reconstruct the entire input mode spectrum, resulting in reduced dynamics.

Subsampled data imposes more difficulties to each of the considered methods. The conventional methods, LSF and DFT, result in reduced dynamics of the respective mode spectra, where LSF generally underesti-

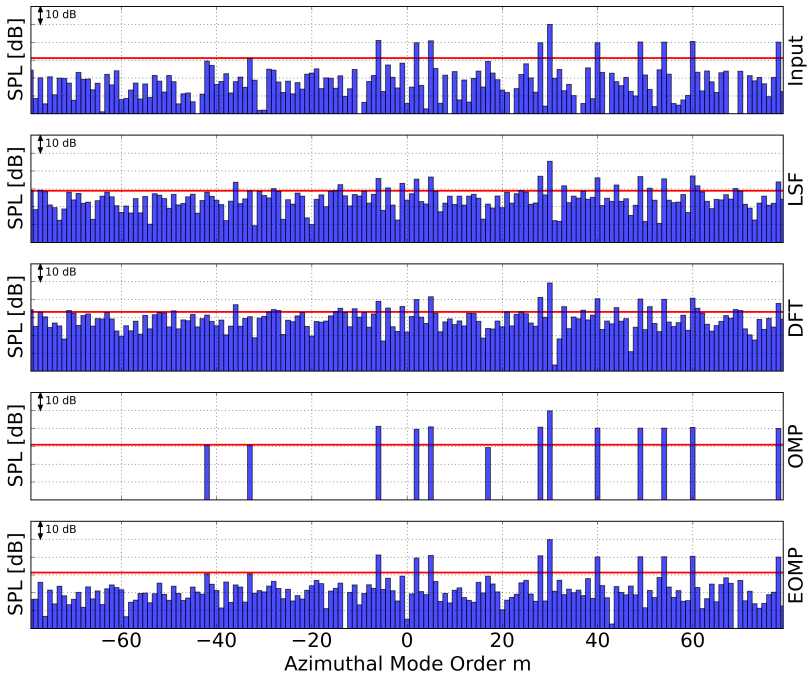

Figure 7. Results of different azimuthal mode analysis methods applied to a simulated pressure data set. The underlying mode spectrum has arbitrary phase relations. For each analysis of the sound field consisting of $M = 159$ azimuthal modes the same sensor array consisting of $K = 100$ unequally spaced sensors was used.

mates the amplitudes of the dominant modes while preserving a relatively low noise floor and DFT gives the correct amplitude of the most dominant mode while the amplitudes of the other modes deviate significantly from the original mode spectrum. Applying Compressed Sensing yields the correct mode amplitudes for the dominant modes and deploying an additional deconvolution step also the noise-related mode amplitudes are estimated well. In this case Compressed Sensing and particularly the EOMP-method allow the analysis of significantly subsampled sound fields and estimation of the complete mode amplitude vector. Furthermore, Compressed Sensing based AMA is not affected by side lobes which will be discussed further in the following section.

IV.A.2. Reconstruction of mode spectra with specific phase relations

The considered methods for AMA are affected by the coherence between modes, i.e. modes with particular phase relations, in different ways. Figures 8 and 9 present analysis results of mode spectra with specific phase relations for a subsampled and oversampled configuration, respectively, using the previously applied CMD-array with non-uniformly spaced sensors. The input spectra are designed such that the side lobe patterns of the two dominant modes interfere destructively resp. constructively. For reasons of clarity the results for the OMP-algorithm without the additional deconvolution step are omitted.

As in the previous section, the LSF-method yields the exact mode amplitudes in the case of oversampling and proves to be unaffected by the phase relations of the dominant modes. Also the Compressed Sensing based AMA performs well showing only small deviations for the amplitudes of the noise-related modes. Thus, both methods can be considered as generally applicable to wide range of mode spectra if the sound field is oversampled. The DFT-method suffers from the occurrence of side lobes and amplitudes of the noise-related modes vary up to 25 dB.

Subsampling the sound field, the LSF- and the DFT-method show the described characteristics of the occurrence of side lobes and the decreased amplitudes of the dominant modes in case of the LSF-method. Interestingly, both methods are affected by particular phase relation between dominant modes and show comparable deviations. The determined amplitudes of individual modes can fluctuate by more than 30 dB.

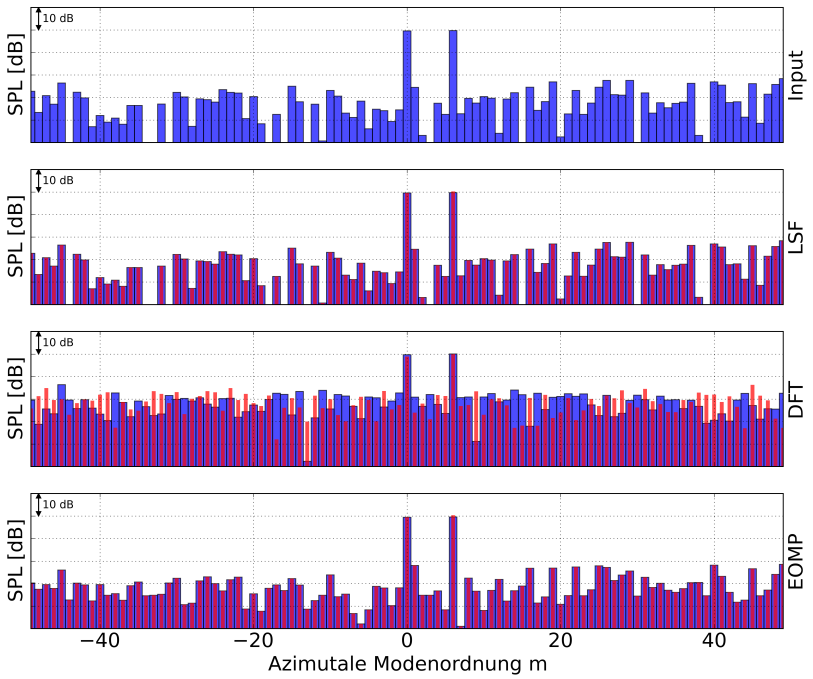

Figure 8. Results of different azimuthal mode analysis methods applied to a simulated pressure data set. The specific phase relation between the dominant modes results in destructive (blue bars) resp. constructive (red bars) interference of the side lobe patterns of both modes. For each analysis of the sound field consisting of $M = 99$ azimuthal modes the same sensor array consisting of $K = 100$ unequally spaced sensors was used.

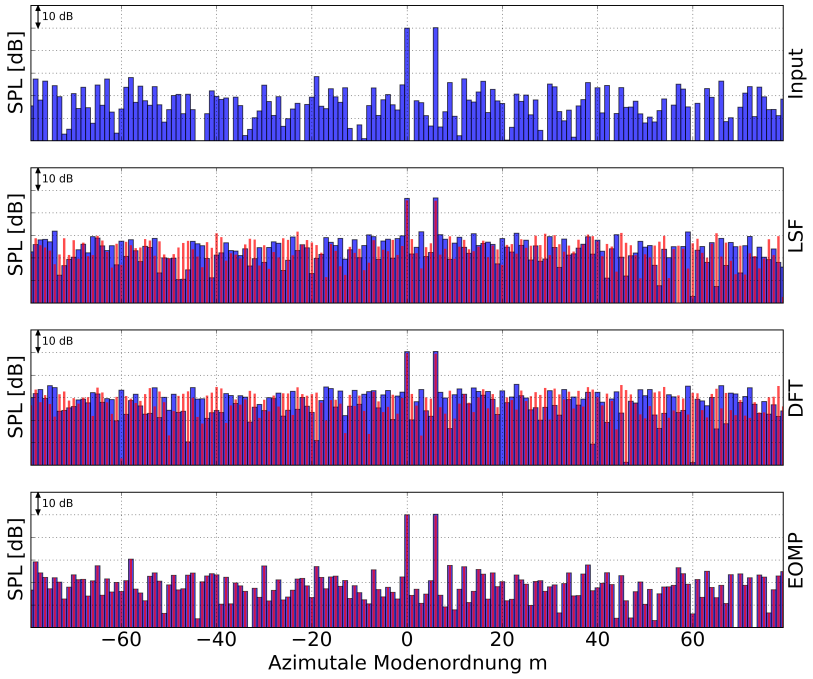

Figure 9. Results of different azimuthal mode analysis methods applied to a simulated pressure data set. The specific phase relation between the dominant modes results in destructive (blue bars) resp. constructive (red bars) interference of the side lobe patterns of both modes. For each analysis of the sound field consisting of $M = 159$ azimuthal modes the same sensor array consisting of $K = 100$ unequally spaced sensors was used.

In contrast, the results of the Enhanced OMP-method do not differ for both cases and show again a good agreement with the original mode spectrum.

The fact that the presented approach can be applied to the analysis of mode spectra with arbitrary or specific phase relations is based on the deconvolution property of the Enhanced OMP-method. Thereby the side lobe patterns of the determined modes are removed from the mode spectrum successively.

IV.B. Application to measured data

The presented method has been applied to measurement data, which was acquired at the UFFA test rig of AneCom AeroTest in Wildau, Germany. The array was situated in the downstream by-pass duct of a scaled Fan stage as depicted in figure 5. The circumferential sensor array consisted of $K = 100$ microphones at non-equidistant positions. For the comparison of the presented method with the conventional methods analyses have been performed for three different tonal components with modal ranges leading to oversampled (see figures 10 and 11) as well as subsampled measurements (see figure 12). The focus of the following study is on the analysis of the results by incorporating the observations from the analyses of simulated data.

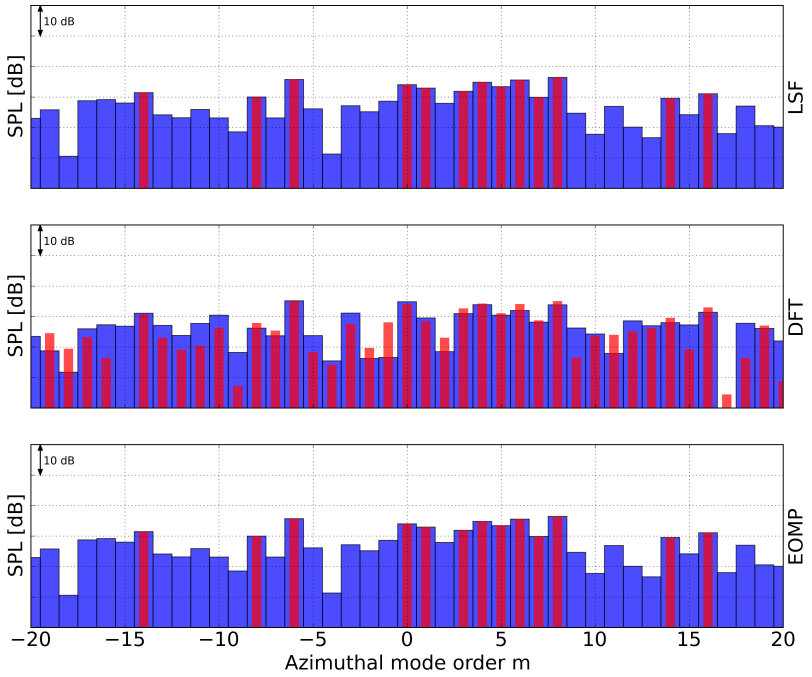

Figure 10. Results of different azimuthal mode analysis methods applied to a measured pressure data set. For each analysis of the sound field the same sensor array consisting of $K = 100$ unequally spaced sensors was used. The maximum azimuthal mode order of propagating modes is $|m_{max}| = 20$. The blue bars indicate the mode amplitudes underlying the measured pressure data. Analysis results of a simulated sound field consisting of the 13 strongest modes are given by the red bars.

Figure 10 shows the analysis results of the measured data and of simulated data consisting of the 13 strongest modes which are identified in the measurement data using OMP. The measurement results are conform with the observations from the analyses of the simulated data in the way, that the LSF- and EOMP-method yield the same results and it can be assumed that the reconstructed mode spectra are free of any artefacts caused by the algorithms. Note, that the LSF-method is applied to perform the deconvolution step in the EOMP-method, because the sound field is oversampled. In contrast to this, the results of the DFT-method differ significantly from the other results due to the occurring side lobes. The superposed side lobe patterns of the 13 strongest modes are depicted by the red bars. It can be seen, that at certain mode orders the amplitudes of the side lobes have a similar magnitude as the respective mode constituents. In table 1 the effect of the interference between the modes and the side lobes is investigated for specific mode orders. Therefore, the complex amplitude of the resulting side lobe due to the considered modes is denoted as $A_{m,SL}$ for mode order m. For the case shown in figure 10 the mode-side lobe interference is

investigated for mode orders $m = \{-2, -1, 2\}$. The phase differences between the three considered modes and the respective side lobes $\angle(A_{m,SL}, A_{m,EOMP})$ reveal destructive interference which results in the level differences $\Delta\mathrm{SPL}(A_{m,SL}, A_{m,EOMP})$ defined by:

$$\mathrm{SPL}(A_{m,SL}, A_{m,EOMP}) = 10 \cdot \log_{10}\left(\frac{|A_{m,EOMP} + A_{m,SL}|}{|A_{m,EOMP}|}\right). \tag{16}$$

However, the level differences due to the mode-side lobe interference do not exactly match the total level differences $\Delta\mathrm{SPL}(A_{m,DFT}, A_{m,EOMP}) = \mathrm{SPL}_{m,DFT} - \mathrm{SPL}(A_{m,EOMP}$. Taking an even wider range of strong modes into consideration for the analysis of the resulting side lobe pattern may improve the match of the level differences as can be seen for the following analyses.

Table 1. Effect of the interference between particular modes and the side lobes present in the analysis of pressure data using the DFT-method on a non-uniform circumferential sensor array.

Figure	Mode order m	$\Delta\mathrm{SPL}(A_{m,DFT}, A_{m,EOMP})$	$\angle(A_{m,SL}, A_{m,EOMP})$	$\Delta\mathrm{SPL}(A_{m,SL}, A_{m,EOMP})$
	[]	[dB]	[°]	[dB]
10	-2	-12.0	-187.2	-17.4
10	-1	-8.9	214.1	-4.0
10	2	-9.4	186.0	-7.2
11	-9	9.9	-39.6	9.9
11	-5	18.5	-228.6	18.5
12	0	-6.9	153.1	-6.9

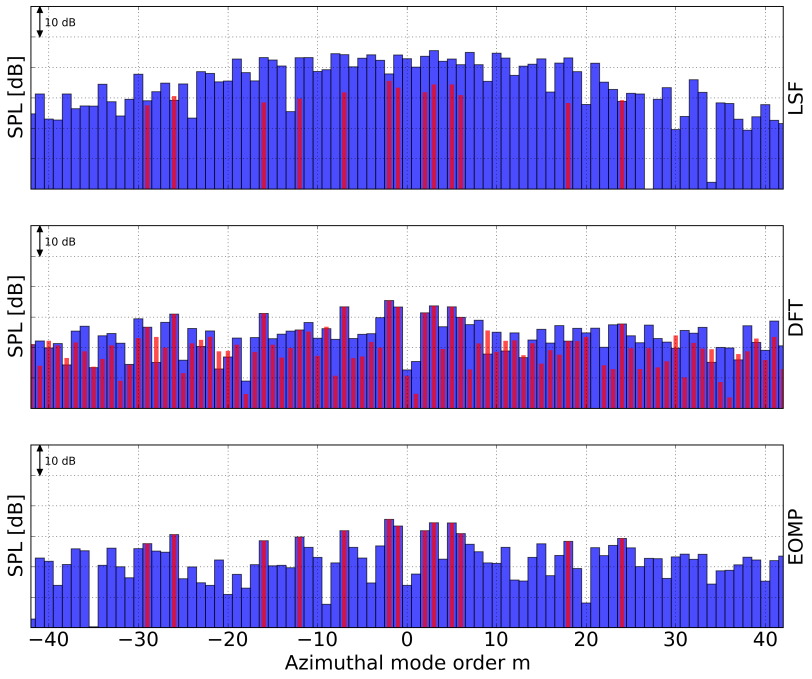

Figure 11. Results of different azimuthal mode analysis methods applied to a measured pressure data set. For each analysis of the sound field the same sensor array consisting of $K = 100$ unequally spaced sensors was used. The maximum azimuthal mode order of propagating modes is $|m_{max}| = 42$. The blue bars indicate the mode amplitudes underlying the measured pressure data. Analysis results of a simulated sound field consisting of the 13 strongest modes are given by the red bars.

For the second analysis, a modal range with $M = 83$ modes is considered and the sound field is oversampled. However, the LSF-method yields largely increased mode amplitudes for lower azimuthal mode orders. This behavior is caused by the bad condition of the system matrix $\boldsymbol{W}$ which occurs for the used array as the

number of modes M approaches the number of sensors K. The results of the DFT-method are corrupted by artifacts of the algorithm, i.e. the occurring side lobes and the interference of the side lobe patterns of the strongest modes as can be seen from the exemplary analysis for mode orders $m = \{-9, -5\}$ in table 1. In contrast to the previous analysis, constructive interference of the respective modes and side lobes yields level differences $\Delta\mathrm{SPL}(A_{m,DFT}, A_{m,EOMP})$ up to 18.5 dB. Interestingly, taking the 13 strongest modes into consideration for the analysis of the mode-side lobe interference yields the matching level differences, so that the difference between mode amplitudes determined by the DFT- and EOMP-methods is fully explained in this case. Based on these and the previous observations Compressed Sensing based AMA can be regarded as stable, even if the system matrix is badly conditioned, and not significantly corrupted by the occurrence of side lobes. Note, that the stability of EOMP was ensured by deploying the DFT-method for the deconvolution step due to the bad condition of the system matrix.

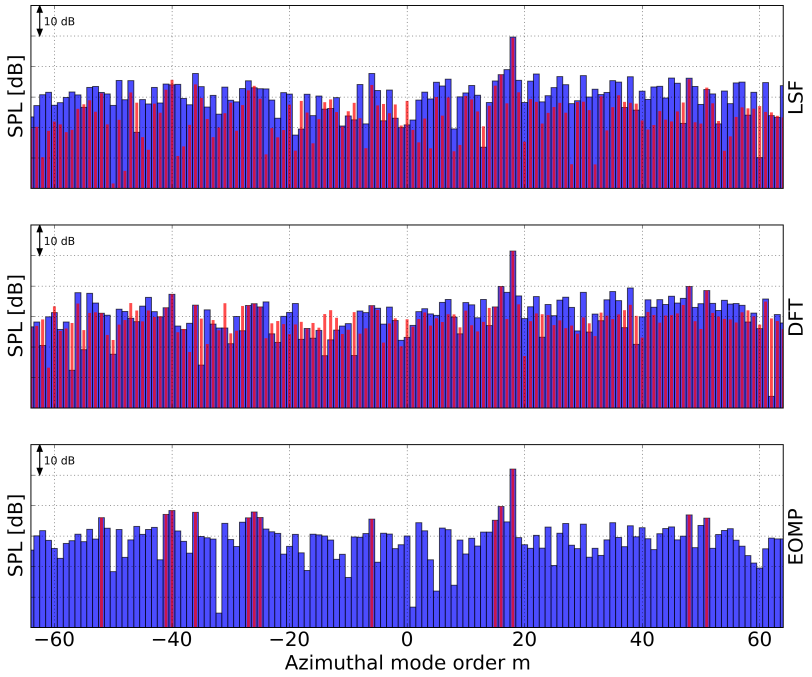

Figure 12. Results of different azimuthal mode analysis methods applied to a measured pressure data set. For each analysis of the sound field the same sensor array consisting of $K = 100$ unequally spaced sensors was used. The maximum azimuthal mode order of propagating modes is $|m_{max}| = 64$. The blue bars indicate the mode amplitudes underlying the measured pressure data. Analysis results of a simulated sound field consisting of the 13 strongest modes are given by the red bars.

Finally, a configuration, where the sound field is subsampled, is analysed and the results are shown in figure 12. The modal range consists of $M = 129$ modes. The reconstructed mode spectra contain a dominant mode at $m = 18$ and modes with levels about 25 dB below the dominant mode. The previous observations regarding the increased mode amplitudes for the DFT-method and the offset of the dominant mode amplitude for the LSF-method are noticeable in the analysis results. Compressed Sensing based AMA reconstructs the dominant mode amplitude with the same level as the DFT-method. The analysis of mode-side lobe interference is performed for mode order $m = 0$. The phase difference given in table 1 indicates that the respective mode interferes destructively with the resulting side lobe of the 13 strongest modes. Also in this case the level difference between the results of the DFT- and EOMP-method can be explained by occurring mode-side lobe interference. However, due to the fact that the sound field is subsampled, the DFT-method is applied for the deconvolution step in the EOMP-method. Generally it can be stated, that with larger modal ranges the impact of side lobes occurring at the deconvolution step of the EOMP-method increases and the accuracy of the resulting mode spectra may be reduced.

V. Conclusion

The present study introduces a new approach for the Azimuthal Mode Analysis based on Compressed Sensing. It is shown that the method gives very accurate results for a wide range of input mode spectra and is very versatile regarding the analysis of over- and subsampled sound fields. By incorporation of a deconvolution step in the Compressed Sensing approach it is possible to reconstruct the entire mode spectrum under consideration. Furthermore, two approaches for the optimisation of array designs in the context of Compressed Sensing are introduced. Deploying the presented optimisation strategies the application of Compressed Sensing based AMA provides the possibility to use smaller sensor arrays or to analyse at higher frequencies without loss of analysis precision compared to the conventional methods least-square fit and Discrete Fourier Transform. The analyses of different, simulated resp. measured pressure data sets show that the Compressed Sensing based AMA is a robust method and not significantly corrupted by the occurrence of side lobes in contrast to the Discrete Fourier-Transform. The experimental data was measured using a circumferential sensor array with non-uniform sensor spacing at a large-scale fan test rig and consists of the tonal components of the sound field of a rotor-stator stage measured in the downstream by-pass duct.

VI. Acknowledgments

THE work presented in this paper is carried out in the national project LIST (Das Leise Installierte Triebwerk), which is supported within the German Luftfahrtforschungsprogramm V by the German Federal Ministry for Economic Affairs and Energy. The authors acknowledge the provision of measurement data by Rolls-Royce Deutschland Ltd & Co.KG which was obtained within the project OPAL, funded by the federal state government of Brandenburg, Germany. The data analysed in this study was published already by Tapken et al.[18].

References

[1]Moore, C., "In-duct investigation of subsonic fan 'rotor alone' noise," *Journal of the Acoustical Society of America*, Vol. 51, 1972, pp. 1471–1482.

[2]Tapken, U. and Enghardt, L., "Optimisation of sensor arrays for radial mode analysis in flow ducts," *12 th AIAA/CEAS Aeroacoustics Conference*, Cambrigde, Massachusetts (USA), May 2006, pp. AIAA 2006–2638.

[3]Rademaker, E., Sijtsma, P., and Tester, B., "Mode detection with an optimised array in a model turbofan engine intake at varying shaft speeds," *7th AIAA/CEAS Aeroacoustics Conference*, Maastricht, The Netherlands, May 2001, pp. AIAA 2001–2181.

[4]Tapken, U., Raitor, T., and Enghardt, L., "Tonal Noise Radiation from an UHBR Fan - Optimized In-Duct Radial Mode Analysis," *15th AIAA/CEAS Aeroacoustics Conference*, Miami, Florida (USA), May 2009, pp. AIAA 2009–3288.

[5]Huang, X., "Compressive Sensing and Reconstruction in Measurements with an Aerospace Application," *AIAA Journal*, Vol. 51, No. 4, April 2013, Technical Notes.

[6]Lengani, D., Kindermann, S., Selic, T., Marn, A., and Heitmeir, F., "Measurement and decomposition of periodic flow structures downstream of a test turbine," *Experiments in Fluids*, Vol. 55:1632, 2014.

[7]Köhler, W., "The Influence of the TCS on the Circumferential Mode Distribution in the Inlet of a Fanrig (UFFA)," *ASME Turbo Expo*, Copenhagen, Denmark, June 2012, pp. GT2012–69762.

[8]Mugridge, B., "The measurement of spinning acoustic modes generated in an axial flow fan," *Journal of Sound and Vibration*, Vol. 10, No. 2, 1969, pp. 227–246.

[9]Tapken, U., Bauers, R., Arnold, F., and Zillmann, J., "Turbomachinery Exhaust Noise Radiation Experiments - Part 2: In-Duct and Far-Field Mode Analysis," *14th AIAA/CEAS Aeroacoustics Conference*, Vancouver, Canada, May 2008, pp. AIAA 2008–2858.

[10]Sijtsma, P. and Zillmann, J., "In-duct and far-field mode detection techniques," *13th AIAA/CEAS Aeroacoustics Conference*, Roma, Italy, May 2007, pp. AIAA 2007–23439.

[11]Tyler, J. M. and Sofrin, T. G., "Axial Flow Compressor Noise Studies," *SAE Transactions*, Vol. 70, 1962, pp. 309–332.

[12]Eldar, Y. and Kutyniok, G., editors, *Compressed Sensing: Theory and Application*, Cambridge University Press, Cambridge, 2012.

[13]Candes, E., Romberg, J., and Tao, T., "Robust Uncertainty Principles: Exact Signal Reconstruction from Highly Incomplete Frequency Information," *IEEE Transactions on Information Theory*, Vol. 52, No. 2, 2006, pp. 489–509.

[14]Donoho, D. L., "Compressed Sensing," *IEEE Transactions on Information Theory*, Vol. 52, No. 4, 2006, pp. 1289–1306.

[15]Tropp, J. A., Romberg, J., and Tao, T., "Signal Recovery from Random Measurements via Orthogonal Matching Pursuit," *IEEE Transactions on Information Theory*, Vol. 53, No. 12, 2007, pp. 4655–4666.

[16]Carin, L., Liu, D., and Guo, B., "Coherence, Compressive Sensing and Random Sensor Arrays," *IEEE Antennas and Propagation Magazine*, Vol. 53, No. 4, 2011.

[17]Xia, P., Zhou, S., and Giannakis, G. B., "Achieving the Welch Bound with Difference Sets," *IEEE Transactions on Information Theory*, Vol. 51, No. 4, 2005.

[18]Tapken, U., Bauers, R., Neuhaus, L., Humphreys, N., Wilson, A., Stöhr, C., and Beutke, M., "A New Modular Fan Rig Noise Test and Radial Mode Detection Capability," *17th AIAA/CEAS Aeroacoustics Conference*, Portland, Oregon (USA), June 2011, pp. AIAA 2011–2897.